Electronic Supplementary Material (ESI) for RSC Advances.

Supporting information

Enantioselectively bioreductive preparation of chiral halohydrins employing two newly identified stererocomplementary reductases

Guo-chao Xu,[1,2] Hui-lei Yu,[1,*] Yue-peng Shang,[1] Jian-he Xu[1]

[1] *State Key Laboratory of Bioreactor Engineering, East China University of Science and Technology, and Shanghai Collaborative Innovation Center for Biomanufacturing Technology, Shanghai 200237, China.*

[2] *The Key Laboratory of Industrial Biotechnology, Ministry of Education, School of Biotechnology, Jiangnan University, Wuxi 214122, China.*

[*] *Corresponding authors. E-mail: huileiyu@ecust.edu.cn; jianhexu@ecust.edu.cn.*

Table S1 Typical sequence motifs of SDR and AKR superfamily found in *Dh*CR and *Cg*CR.

Typical sequence motifs of SDR found in *Dh*CR[a]			
Sequence motif of SDR	**Function**	**Position in SDR**	**Position in *Dh*CR**
(T)Gxx(x)Gx(G)xA[b]	Coenzyme binding region, maintenance of central *β*-sheet	12–21	40–49
D	Stabilization of adenine ring pocket, weak binding to coenzyme	60	94
S, YxxxK	Catalytic triad	138, 151–155	172, 187–191
N	Connection of substrate binding loop and active site	179	212
PG	Reaction direction	183–184	216–217
T	H-bonding to carboxamide of nicotinamide ring	188	221
Typical sequence motifs of AKR found in *Cg*CR[c]			
Sequence motif of AKR	**Function**	**Position in AKR**	**Position in *Cg*CR**
G, G, G, D, P, G, P	Stabilization of the barrel core	20, 22, 45, 112, 119, 164, 186	23, 25, 45, 106, 113, 165, 187
A, W	Substrate binding	52, 118	52, 112
D, Y, K, H	Catalytic tetrad	50, 55, 84, 117	50, 55, 80, 111
N, Q	H-bonding with carboxamide moiety of the cofactor	167, 190	168, 191
T, D	Interaction with nicotinamide ribose ring of the cofactor	23, 50	26, 50
S, R	H-bonding to adenosine 2'-monophosphate of the cofactor	271, 276	263, 268

[a] (Positions refers to residue numbering as in 3*β*/17*β*-hydroxysteroid dehydrogenases (PDB: 1HXH); [b] x represents any amino acids; [c] Positions refers to residue numbering as in 3*α*-hydroxysteroid dehydrogenases (PDB: 1RAL).

Table S2 The secondary structure elements motif in ‘classical’ SDR, ‘extended’ SDR and *Dh*CR.

Secondary structure element	Conserved SDR motifs			Function	Position in *Dh*CR
	Classical	Extended	*Dh*CR		
β1+α1	TGxxxGhG	TGxxGhaG	TGSSGGIG	Coenzyme binding region	β1+α1
β3+α3	Dhx[cp]	DhxD	DPED	Adenine ring binding of coenzyme	β3+α3
β4	GxhDhhhNNAGh	[DE]xhhHXAA	GTIDVFVANAGV	Structural role in stabilizing central β-sheet	β4
β5	GxhhxhSSh	hhhxSSxxhaG	GSLVLTASMSG	Part of active site	β5
α5	Yx[AS][ST]K	PYxx[AS]Kxxh	PYNAAKAGV	Part of active site	α6
β6	H[KR]h[NS]xhxPGxxxT	h[KR]xxNGP	ARVNTISPGYIAT	Structural role, reaction direction	β6

*In the motifs, ‘a’ denotes an aromatic residues, ‘c’ a charged residue, ‘h’ a hydrophobic residue, ‘p’ a polar residue and ‘x’ any residue. Conserved amino acids are underlined. Alternative amino acids at a motif position are given within brackets. The secondary elements of classical and extended SDR are based on 3α/20β-hydroxysteroid dehydrogenase (PDB: 2HSD).

Table S3 Steady-state kinetic constants of stererocomplementary *Dh*CR and *Cg*CR.

	*Dh*CR		*Cg*CR	
Substrate	COBE	NADPH	COBE	NADPH
K_M /mM	1.30 ± 0.01	0.035 ± 0.001	3.70 ± 0.08	0.028 ± 0.003
V_{max} /μmol·min^{-1}·mg^{-1}	29.7 ± 0.3	−	42.1 ± 0.6	−
k_{cat} /s^{-1}	16.6 ± 0.3	−	27.9 ± 0.4	−
k_{cat}/K_M s^{-1}·mM^{-1}	12.8	−	7.55	−

Table S4 Substrate specificities of stererocomplementary *Dh*CR and *Cg*CR.

Substrate	*Dh*CR		*Cg*CR	
	Specific activity /U·mg^{-1}	*ee* % / (*R*/*S*)	Specific activity /U·mg^{-1}	*ee* % / (*R*/*S*)
1	0.16	>99 (*R*)	0.32	92 (*S*)
2	0.11	>99 (*R*)	0.12	97 (*S*)
3	0.075	>99 (*R*)	0.17	86 (*S*)
4	2.1	>99 (*S*)	0.58	98 (*R*)
5	6.9	>99 (*S*)	2.0	56 (*R*)
6	0.06	>99 (*R*)	0.19	>99 (*S*)
7	<0.01	*n. d.* [a]	1.0	>99 (*S*)
8	5.3	>99 (*R*)	3.2	96 (*S*)
9	22	>99 (*S*)	2.6	>99 (*R*)
10	0.35	>99 (*S*)	2.4	>99 (*R*)
11	33	>99 (*S*)	2.9	>99 (*R*)
12	0.37	>99 (*R*)	0.28	>99 (*S*)
13	0.087	>99 (*R*)	0.50	>99 (*S*)
14	0.024	>99 (*R*)	0.034	>99 (*S*)
15	1.1	>99 (*R*)	0.15	>99 (*S*)
16	1.4	>99 (*R*)	0.12	>99 (*S*)
17	0.52	>99 (*R*)	0.02	>99 (*S*)
18	0.2	>99 (*R*)	0.01	>99 (*S*)
19	3.0	>99 (*R*)	0.38	>99 (*S*)
20	0.11	>99 (*R*)	0.56	>99 (*S*)
21	0.1	>99 (*R*)	0.64	>99 (*S*)
22	13	>99 (*S*)	8.0	>99 (*R*)
23	0.48	>99 (*S*)	3.8	>99 (*R*)
24	2.7	>99 (*R*)	9.3	>99 (*S*)
25	3.6	>99 (*R*)	19	>99 (*S*)

[a] *n. d.*: no product was detected.

Table S5 Concentrations of NAD^+ and $NADP^+$ in the fresh wet cells and dry cells.

Cell	**NAD^+ /μmol·g^{-1}**	**$NADP^+$ /μmol·g^{-1}**
Fresh wet cells	0.44 ± 0.02	1.03 ± 0.06
Dry cells	0.62 ± 0.02	1.86 ± 0.13

Table S6 Optimization of *Dh*CR and *Cg*CR catalyzed asymmetric reduction of COBE.

Catalyst		Substrate			S/C	Time	Conv.	% *ee*
Name	[g·L^{-1}]	[g]	[M]	[g·L^{-1}]	ratio [b]	[h]	[%]	/(R/S)
*Dh*CR	10	0.33	0.2	33	3.3	6	>99	>99 (*S*)
	20	0.83	0.5	83	4.15	8	>99	>99 (*S*)
	20	1.65	1.0	165	8.25	12	>99	>99 (*S*)
	20	3.30	2.0	330	16.5	24	>99	>99 (*S*)
	20	330 [a]	2.0	330	16.5	24	>99 (92.5) [c]	>99 (*S*)
*Cg*CR	5	0.33	0.2	33	6.6	6	>99	>99 (*R*)
	10	0.86	0.5	83	8.3	6	>99	>99 (*R*)
	10	1.65	1.0	165	16.5	12	>99	>99 (*R*)
	10	3.30	2.0	330	33	24	>99	>99 (*R*)
	10	330 [a]	2.0	330	33	24	>99 (93.0) [c]	>99 (*R*)

[a] Reactions were carried out at 1 L scale with mechanical agitation. [b] S/C ratio: substrate to catalyst ratio. [c] Numbers in the bracket were isolation yield.

Table S7 Comparison of the characteristics of reported enzymes that produce optically active CHBE.

	Enzyme	Family	K_M [mM]	Concn [g·L^{-1}]	Cofactor [mM]	Time [h]	Yield [%]	*ee* [%] /(R/S)	S.T.Y. [g·L^{-1}·d^{-1}]	TTN of cofactor
1	S1 [a]	SDR	4.6	300	0.081	13	96	100 (*S*)	538	21,550
				500 [m]	0.167	34	85	100 (*S*)	304	21,600
2	*Sc*CR [b]	SDR	0.49	600	0.3	22	92	>99 (*S*)	609	12,100
3	*Cm*MR [c]	MDR	–	300	0.13	36	92	91.6 (*S*)	186	12,900
4	*Cm*CR [d]	SDR	–	493.8	0.3	14	99	>99 (*S*)	–	10,000
5	*Ps*CRI [e]	SDR	4.9	230	0.10	30	90	99 (*S*)	168	12,600
6	*Ps*CRII [f]	SDR	3.3	250	0.10	30	91	99 (*S*)	184	13,980
7	CPE [g]	SDR	0.19	3.3	0.25	20	91	>99 (*S*)	3.65	–
8	*Dh*CR [h]	SDR	1.3	660 [n]	0	24	92.5	>99 (*S*)	305	53,800
9	SsCR [i]	AKR	3.8	300	0.13	16	94	91.7 (*R*)	419	13,500
10	YueD [j]	SDR	0.70	215 [n]	1	5	92	99.6 (*R*)	961	1196
11	*Cg*KR1 [k]	MDR	–	330	0	24	89	96.5 (*R*)	297	–
12	*Cg*CR [l]	AKR	3.7	660 [n]	0	12	93.0	>99 (*R*)	614	108,000

[a] *Candida magnolia* (Kizaki et al., 2001), [b] *Streptomyces coelicolor* (Wang et al., 2011), [c] *C. macedoniensis* (Kataoka et al., 2006), [d] *C. magnolia* (He et al., 2014), [e] *Pichia stipites* (Ye et al., 2009), [f] *P. stipites* (Ye et al., 2010), [g] *Candida parapsilosis* (Wang et al., 2012),[h] *D. hansenii* (This work), [i] *Sporobolomyces salmonicolor* (Kataoka et al., 1999), [j] *Bacillus subtilis* (Ni et al., 2011), [k] *Candida glabrata* (Ma et al., 2012), [l] *C. glabrata* (This work), [m] Reaction was carried out in n-butyl acetate/aqueous (1/1) phase (Kizaki et al., 2001), [n] Reactions were carried out in toluene/aqueous (1/1) phase (Wang et al., 2011).

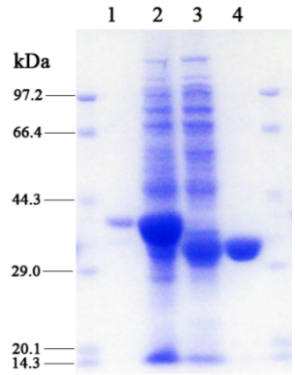

Figure S1 SDS-PAGE analysis of the purified *Cg*CR and *Dh*CR. Lane 1: purified *Cg*CR; Lane 2: crude extract of *Cg*CR; Lane 3: crude extract of *Dh*CR; Lane 4: purified *Dh*CR.

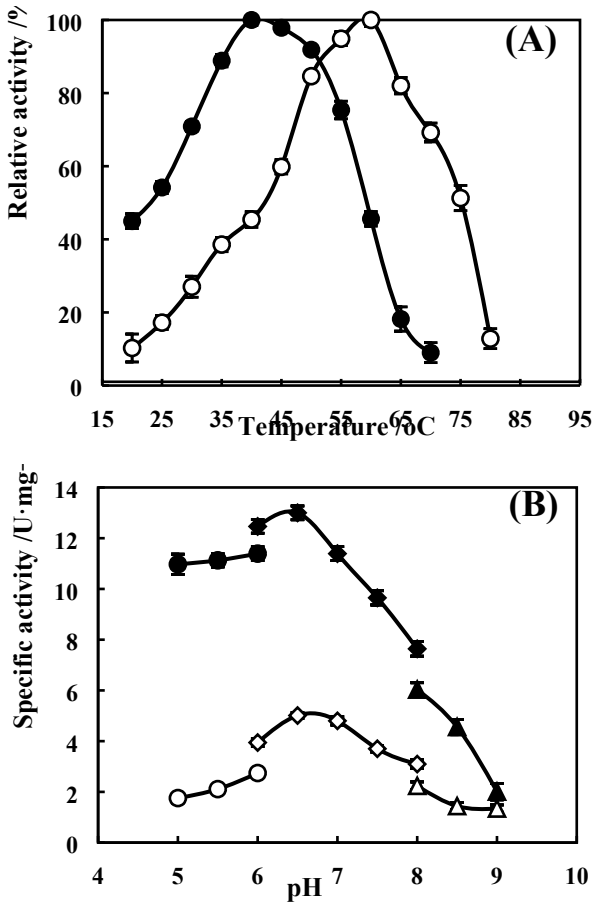

Figure S2 Effect of temperature and pH on the activity of *Dh*CR and *Cg*CR. (A) Temperature-profile of *Dh*CR (●) and CgCR (○); (B) pH-profile of *Dh*CR (solid symbols) and *Cg*CR (Hollow symbols), Cycle: Citrate buffer (pH 5.0–6.0), Diamond: Phosphate sodium buffer (pH 6.0–8.0), and Triangle: Glycine-NaOH buffer (pH 8.0–9.0).

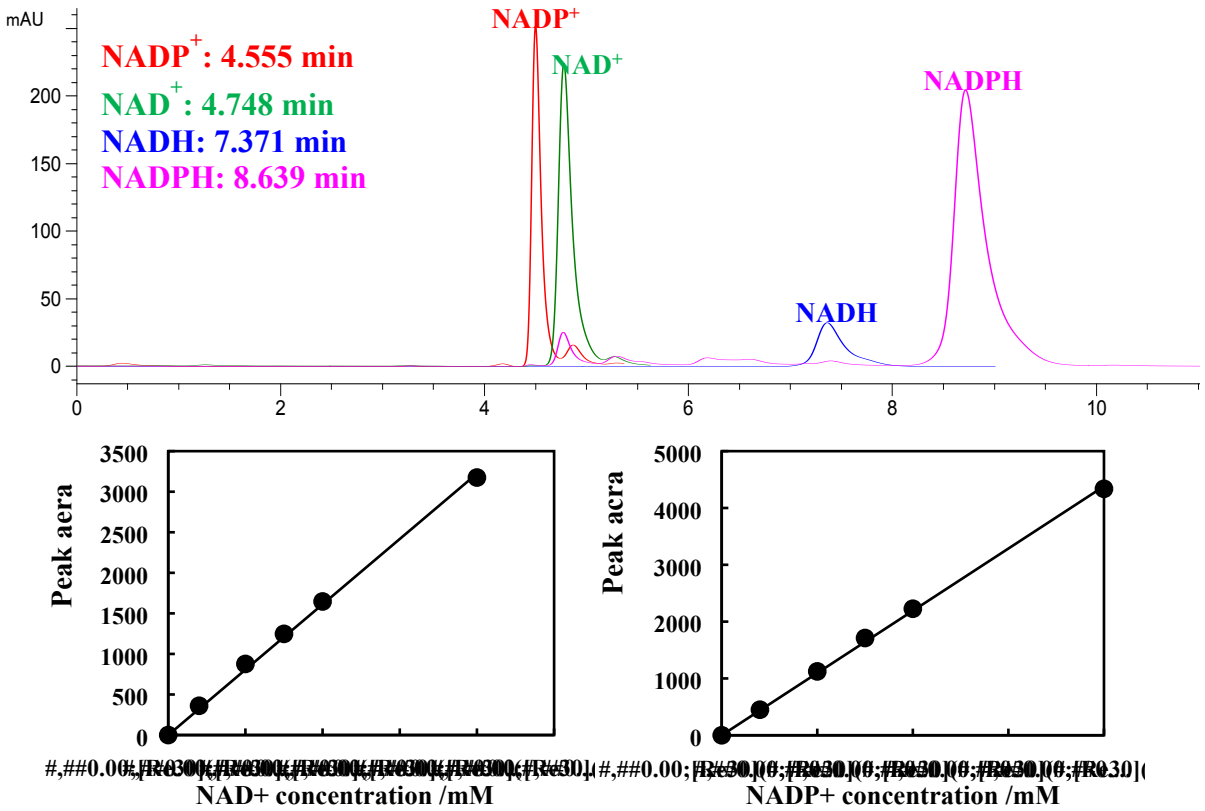

Figure S4 Calibration curves of oxidized cofactors.

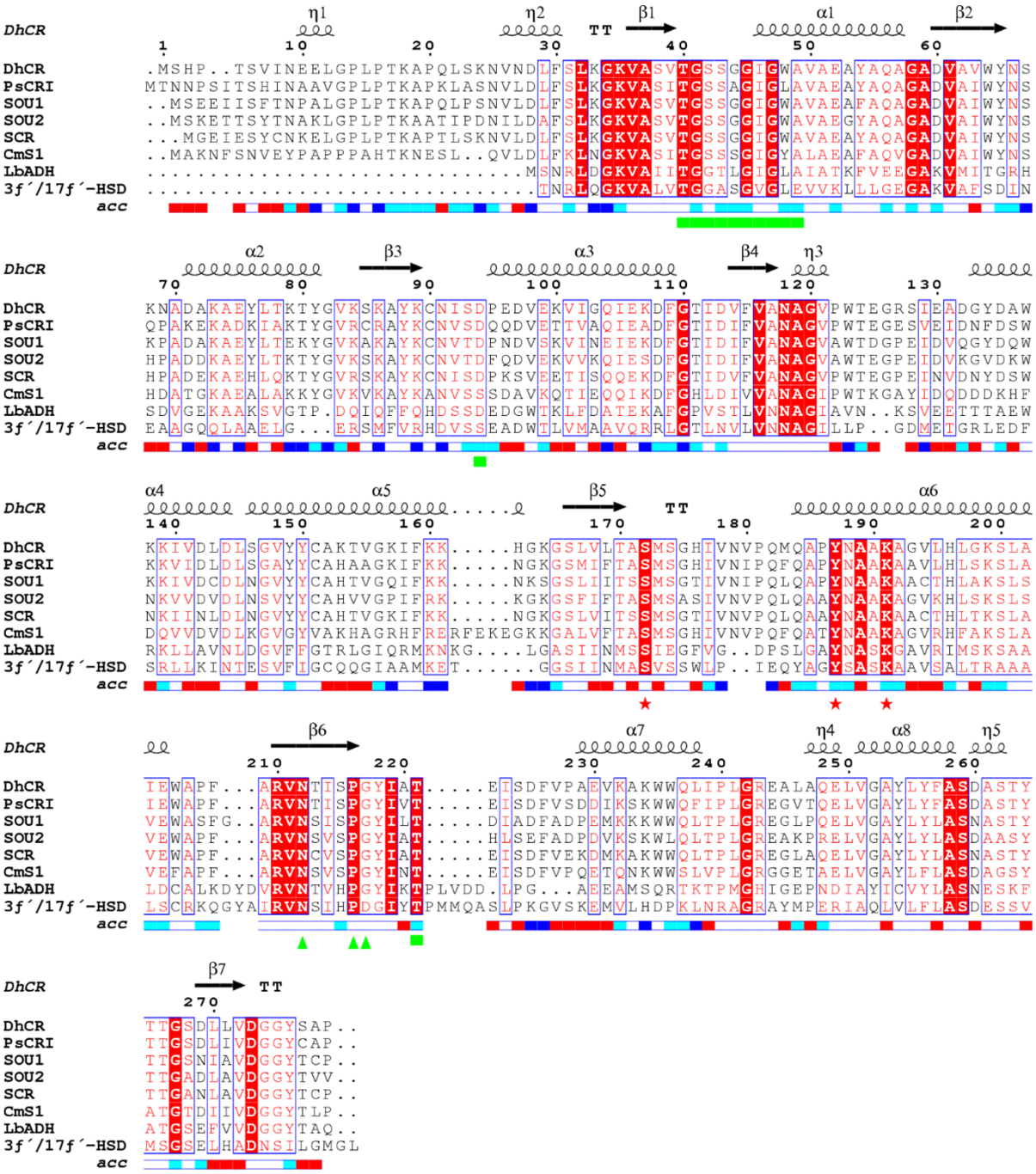

Figure S5 Multiple sequences alignment of *Dh*CR with several SDR members. PsCRI (*Phichia stipites* ATCC58785, A3GF07), SOU1 (*Candida albicans* SC5314, P87219), SOU2 (*Candida albicans* SC5314, P87218), SCR (*Candida parapsilosis*, D5G304), CmS1 (*Candida magnolia*, Q9C4B3), LbADH (*Lactobacillus brevis*, Q84EX5), 3*β*/17*β*-hydroxysteroid dehydrogenase, (*Comamonas testosterone* ATCC11996, H1RW42). ★: catalytic residues; ■: cofactor binding residues; ▲: substrate binding residues.

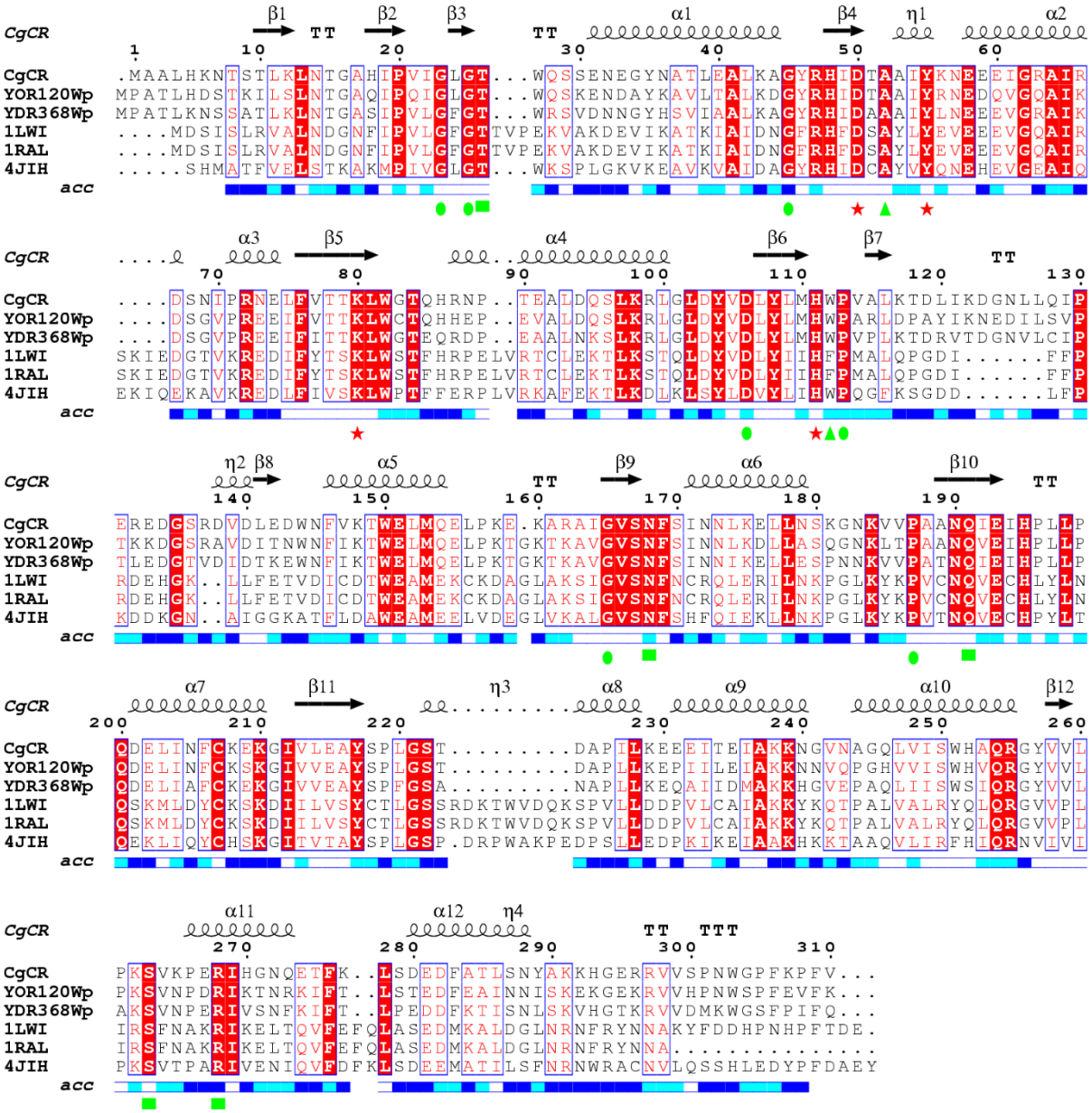

Figure S6 Multiple sequences alignment of *Cg*CR with several AKR members. YOR120Wp (*Saccharomyces cerevisiae* AWRI1631, B5VS12), YOR368Wp (*Saccharomyces cerevisiae* AWRI1631, B5VSP3), 1LWI (3α-hydroxysteroid dehydrogenase, *Rattus norvegicus*, P23457), 1RAL (3α-hydroxysteroid dehydrogenase, *Rattus norvegicus*, Q91WT7), 4JIH (Aldo-keto reductase AKR1B10, *Gorilla*, G3S8S6). ★: catalytic residues; ●: structure-stabilizing residues; ■: cofactor-binding residues; ▲: substrate-binding residues.

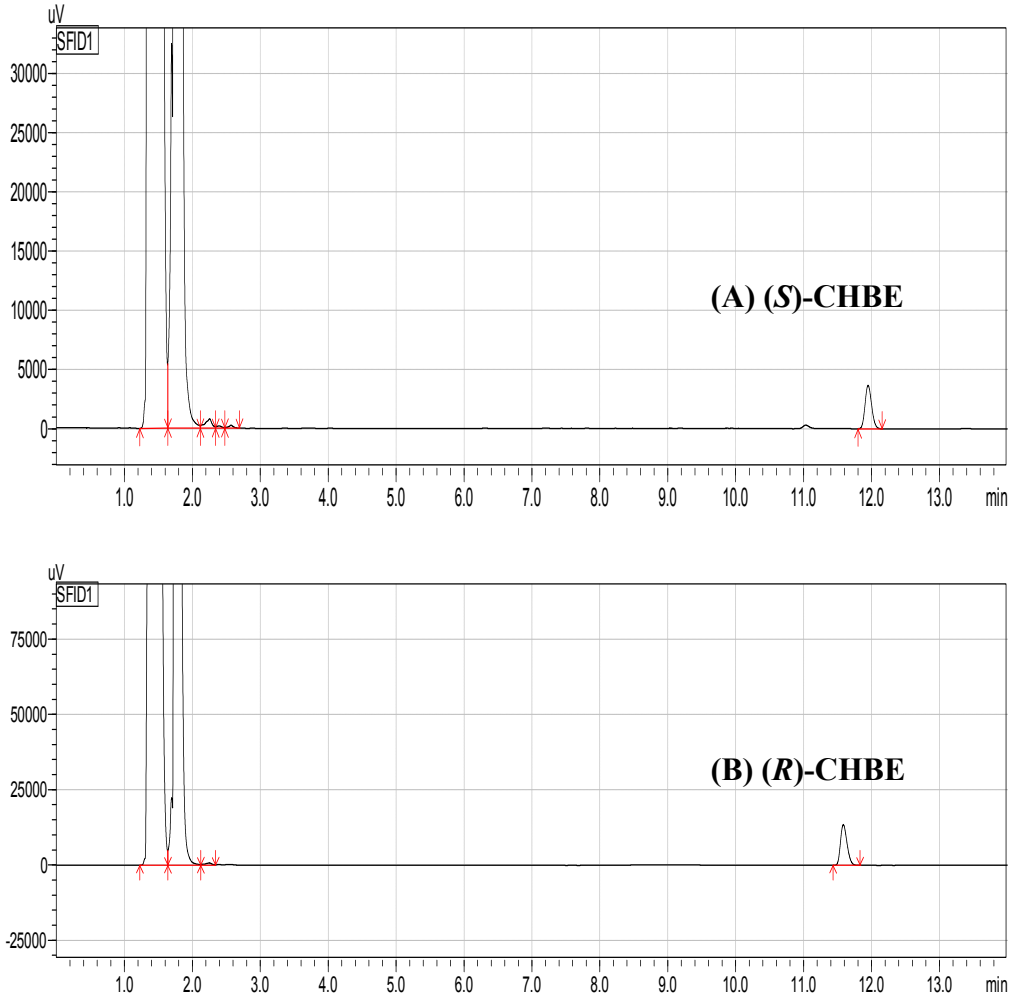

Figure S7 GC spectra of CHBE. (A) Ethylated (*S*)-CHBE produced by *Dh*CR; (B) Ethylated (*R*)-CHBE produced by *Cg*CR.

Reference

Kizaki, N., Yasohara, Y., Hasegawa, J. Wada, M., Kataoka, M., Shimizu, S., 2001. Synthesis of optically pure ethyl (*S*)-4-chloro-3-hydroxybutanoate by *Escherichia coli* transformant cells coexpressing the carbonyl reductase and glucose dehydrogenase genes. Appl. Microbiol. Biotechnol. 55, 590−595.

Kataoka, M., Hoshino-Hasegawa, A., Thiwthong, R., Higuchi, N., Ishige, T., Shimizu, S., 2006. Gene cloning of an NADPH-dependent menadione reductase from *Candida macedoniensis*, and its application to chiral alcohol production. Enzyme Microb. Technol. 38, 944−951.

He, Y.C., Tao, Z.C., Zhang, X., Yang, Z.X., Xu, J.H., 2014. Highly efficient synthesis of ethyl (*S*)-4-chloro-3-hydroxybutanoate and its derivatives by a robust NADH-dependent reductase from *E. coli* CCZU-K14. Bioresour. Technol. 161, 461−464.

Ye, Q., Yan, M., Yao, Z., Xu, L., Cao, H., Li, Z.J., Chen, Y., Li, S.Y., Bai, J.X., Xiong, J., Ying, H.J., Ouyang, P.K., 2009. A new member of the short-chain dehydrogenase/reductases superfamily: purification, characterization and substrate specificity of a recombinant carbonyl reductase from *Pichia stipites*. Bioresour. Technol. 100, 6022−6027.

Ye, Q., Cao, H., Mi, L., Yan, M., Wang, Y., He, Q.T., Li, J., Xu, L., Chen, Y.J., Xiong, J., Ouyang, P.K., Ying, H.J., 2010. Biosynthesis of (*S*)-4-chloro-3-hydroxybutanoate ethyl using *Escherichia coli* co-expressing a novel NADH-dependent carbonyl reductase and a glucose dehydrogenase. Bioresour. Technol. 101, 8911−8914.

Wang, Q.Y., She, L.H., Ye, T.T., Cao, D., Chen, R., Pei, X.L., Xie, T., Li, Y., Gong, W.B., Yin, X.P., 2012. Overexpression and characterization of a novel (*S*)-specific extended short-chain dehydrogenase/reductase from *Candida parapsilosis*. Bioresour. Technol. 123, 690−694.

Kataoka, M., Rohani, L.P., Yamamoto, K., Kawabata, H., Wada, M., Kita, K., Yanase, H., Shimizu, S., 1999. Stereoselective reduction of ethyl 4-chloro-3-oxobutanoate by *Escherichia coli* transformant cells coexpressing the aldehyde reductase and glucose dehydeogenase genes. Appl. Microbiol. Biotechnol. 41, 486−490.

Ni, Y., Li, C.X., Wang, L.J., Zhang, J., Xu, J.H., 2011. Highly stereoselective reduction of prochiral ketones by a bacterial reductase coupled with cofactor regeneration. Org. Biomol. Chem. 9, 5463−5468.

Ma, H.M., Yang, L.L., Ni, Y., Zhang, J., Li, C.X., Zheng, G.W., Yang, H.Y., Xu, J.H., 2012. Stereospecific reduction of methyl *o*-chlorobenzoylformate at 300 $g \cdot L^{-1}$ without addition cofactor using a carbonyl reductase mined from *Candida glabrata*. Adv. Synth. Catal. 354, 1765−1772.

Kizaki, N., Yasohara, Y., Hasegawa, J. Wada, M., Kataoka, M., Shimizu, S., 2001. Synthesis of optically pure ethyl (*S*)-4-chloro-3-hydroxybutanoate by *Escherichia*

coli transformant cells coexpressing the carbonyl reductase and glucose dehydrogenase genes. Appl. Microbiol. Biotechnol. 55, 590−595.